

SPECIAL ISSUE PAPER

New deterministic and stochastic simulation models for non-isotropic scattering mobile-to-mobile Rayleigh fading channels[†]

Xiang Cheng^{1*}, Cheng-Xiang Wang¹, David I. Laurenson², Sana Salous³ and Athanasios V. Vasilakos⁴

¹ Joint Research Institute for Signal and Image Processing, School of Engineering & Physical Sciences, Heriot-Watt University, Edinburgh, EH14 4AS, U.K.

² Joint Research Institute for Signal and Image Processing, Institute for Digital Communications, University of Edinburgh, Edinburgh, EH9 3JL, U.K.

³ Center for Communication Systems, School of Engineering, University of Durham, Durham, DH1 3LE, U.K.

⁴ Department of Computer and Telecommunications Engineering, University of Western Macedonia, GR 50100 Kozani, Greece

ABSTRACT

For the practical simulation and performance evaluation of mobile-to-mobile (M2M) communication systems, it is desirable to develop accurate M2M channel simulation models for more realistic scenarios of non-isotropic scattering. In this paper, by using a ‘double-ring’ concept to describe M2M non-isotropic scattering environments, we propose new deterministic and stochastic sum-of-sinusoids (SoS) based simulation models. The proposed simulation models extensively consider the distributions of the angle of arrival (AoA) and the angle of departure (AoD), and thus provide a good approximation to the desired statistical properties of the reference model. Copyright © 2009 John Wiley & Sons, Ltd.

KEYWORDS

mobile-to-mobile communications; sum-of-sinusoids channel simulator; Rayleigh fading; non-isotropic scattering

*Correspondence

Xiang Cheng, Joint Research Institute for Signal and Image Processing, School of Engineering & Physical Sciences, Heriot-Watt University, Edinburgh, EH14 4AS, U.K.

E-mail: xc48@hw.ac.uk

1. INTRODUCTION

In recent years, mobile-to-mobile (M2M) communications have received increasing attention due to some new applications, such as wireless mobile *ad hoc* networks [1], relay-based cellular networks [2], and dedicated short range communications for intelligent transportation systems (IEEE 802.11p) [3]. Such M2M systems consider that both the transmitter (Tx) and receiver (Rx) are in motion and are equipped with low elevation antennas. To successfully analyze and design such M2M systems, it is necessary to have proper mathematical reference models for the underlying propagation channels. Many M2M mathematical reference models have been proposed for both isotropic scattering environments, e.g., the models in References [4] and [5], and more realistic environments of non-isotropic scattering, e.g., the models in References [6–10].

Besides the modeling of a M2M channel and the investigation of its statistical properties, the development of accurate M2M channel simulation models also plays a major role in the practical simulation and performance evaluation of M2M systems. However, in the literature, most channel simulation models for wireless communications were developed for conventional fixed-to-mobile (F2M) cellular radio systems [11–17]. As mentioned in Reference [18], simulation models for a F2M channel cannot be readily used to simulate a M2M channel due to the differences of their statistical properties. Wang and Cox [19] were the first to propose a simulation model for isotropic scattering M2M Rayleigh fading channels by using the line spectrum filtering method. Due to the application of line spectrum filtering, the model has high complexity and severe performance deficiencies as pointed out in Reference [18]. Therefore, the sum-of-sinusoids (SoS)

[†]This paper was presented in part at *VehiCom'09, co-located with IWCMC'09*, Leipzig, Germany, 21–24 June 2009.

method was used in References [18] and [20] to develop better isotropic scattering M2M Rayleigh fading simulation models. Generally speaking, the SoS method allows us to approximate the underlying random fading processes by the superposition of a finite number of properly weighted harmonic functions. An SoS based simulation model can be either deterministic or stochastic in terms of the underlying parameters (gains, frequencies, and phases) [16]. For a deterministic model, all the parameters are fixed for all simulation trials. In contrast, a stochastic model has at least one parameter (gains and/or frequencies) as a random variable which varies for each simulation trial. Therefore, the relevant statistical properties of a stochastic model vary for each simulation trial but converge to the desired ones when averaged over a sufficient number of trials. In Reference [18], the authors used the ‘double-ring’ concept to derive two SoS based simulation models (deterministic and stochastic models) for isotropic scattering M2M channels. The stochastic model in Reference [18] was further improved in Reference [20] by choosing orthogonal functions for in-phase and quadrature components of the complex fading envelope. More recently, in Reference [21] the Rayleigh M2M stochastic simulation model in Reference [18] was extended to include a line-of-sight component, i.e., for Ricean fading channels. However, it is worth noting that all the aforementioned simulation models limit their applications to isotropic scattering environments. The simulation models for M2M Rayleigh fading channels under a more realistic scenario of non-isotropic scattering are scarce in the current literature.

To the best of the authors’ knowledge, only one stochastic SoS based simulation model [22] has been proposed for the simulation of non-isotropic scattering M2M Rayleigh fading channels. However, this model only considered the symmetrical property of the distributions of the angle of arrival (AoA) and angle of departure (AoD) and was designed based on the acceptance rejection algorithm (ARA). This leads to the ARA model having a notable difficulty in reproducing the desired statistical properties of the reference model and a comparatively high computational complexity. Furthermore, it is worth noting that accurate deterministic simulation models for non-isotropic scattering M2M Rayleigh fading channels are not available in the current literature.

To fill the above gap, in this paper, based on the ‘doubling’ concept in Reference [18], we first propose a new M2M deterministic SoS based simulation model. By allowing at least one parameter (frequencies and/or gains) to be a random variable, our deterministic model can be further modified to be a stochastic model. It is worth noting that the proposed simulation models incorporate the probability density functions (PDFs) of the AoA and AoD, and thus can approximate the desired statistical properties of the reference model for any non-isotropic scattering M2M Rayleigh fading channel. Moreover, compared to the ARA stochastic model in Reference [22], our stochastic model presents better approximation to the desired properties of the reference model with an even smaller number of harmonic functions.

The paper is structured as follows. Section 2 gives a brief description of the reference model for non-isotropic scattering M2M Rayleigh fading channels. In Section 3, we propose two new SoS based simulation models (deterministic and stochastic models). The performance evaluation of our models is presented in Section 4. Finally, conclusions are drawn in Section 5.

2. REFERENCE MODEL

Using Akki and Haber’s mathematical model [4] and considering the directions of movement of the Tx and Rx, we can express the complex fading envelope of our reference model, under a narrowband non-isotropic scattering M2M Rayleigh fading assumption, as

$$h(t) = h_i(t) + jh_q(t) = \lim_{N \rightarrow \infty} \frac{1}{\sqrt{N}} \sum_{n=1}^N e^{j\psi_n} e^{j[2\pi f_{T_{\max}} t \cos(\phi_T^n - \gamma_T) + 2\pi f_{R_{\max}} t \cos(\phi_R^n - \gamma_R)]} \quad (1)$$

where $h_i(t)$ and $h_q(t)$ are in-phase and quadrature components of the complex fading envelope $h(t)$, respectively, $j = \sqrt{-1}$, N is the number of harmonic function representing propagation paths (effective scatterers), $f_{T_{\max}}$ and $f_{R_{\max}}$ are the maximum Doppler frequency due to the motion of the Tx and Rx, respectively. The Tx and Rx move in directions determined by the angles of motion γ_T and γ_R , respectively. The random AoA and AoD of the n th path are denoted by ϕ_R^n and ϕ_T^n , respectively, and ψ_n is the random phase uniformly distributed on $[-\pi, \pi)$. It is assumed that ϕ_R^n , ϕ_T^n , and ψ_n are mutually independent random variables.

Since the number N of effective scatterers in the reference model $h(t)$ tends to infinity, the discrete expressions of the AoA $\phi_R^{(n)}$ and AoD $\phi_T^{(n)}$ can be replaced by the continuous expressions ϕ_R and ϕ_T , respectively. Note that since $h(t)$ describes a non-isotropic scattering M2M Rayleigh fading channel, the AoA ϕ_R and AoD ϕ_T exhibit non-uniform distributions. In the literature, many different non-uniform distributions have been proposed to characterize the AoA ϕ_R and AoD ϕ_R , such as Gaussian, wrapped Gaussian, and cardioid PDFs [23]. In this paper, the von Mises PDF [24] is used, which can approximate all the aforementioned PDFs and match well the measured data in References [7] and [24]. The von Mises PDF is defined as $f(\phi) \triangleq \exp[k \cos(\phi - \mu)] / [2\pi I_0(k)]$, where $\phi \in [-\pi, \pi)$, $I_0(\cdot)$ is the zeroth-order modified Bessel function of the first kind, $\mu \in [-\pi, \pi)$ accounts for the mean value of the angle ϕ , and k ($k \geq 0$) is a real-valued parameter that controls the angle spread of the angle ϕ . For $k = 0$ (isotropic scattering), the von Mises PDF reduces to the uniform distribution, while for $k > 0$ (non-isotropic scattering), the von Mises PDF approximates different distributions based on the values of k [24]. Applying

the von Mises PDF to the AoA ϕ_R and AoD ϕ_T , we obtain $f(\phi_R) \triangleq \exp[k_R \cos(\phi_R - \mu_R)]/[2\pi I_0(k_R)]$ and $f(\phi_T) \triangleq \exp[k_T \cos(\phi_T - \mu_T)]/[2\pi I_0(k_T)]$, respectively.

The autocorrelation function (ACF) of the reference model $h(t)$ can be expressed as [10]

$$\begin{aligned} \rho_{hh}(\tau) &= \mathbf{E} [h(t) h^*(t - \tau)] \\ &= \frac{1}{I_0(k_T) I_0(k_R)} I_0 \left[(A_T^2 + B_T^2)^{1/2} \right] \\ &\quad \times I_0 \left[(A_R^2 + B_R^2)^{1/2} \right] \end{aligned} \quad (2)$$

with

$$A_T = k_T \cos(\mu_T) + j2\pi\tau f_{T_{\max}} \cos(\gamma_T) \quad (3a)$$

$$B_T = k_T \sin(\mu_T) + j2\pi\tau f_{T_{\max}} \sin(\gamma_T) \quad (3b)$$

$$A_R = k_R \cos(\mu_R) + j2\pi\tau f_{R_{\max}} \cos(\gamma_R) \quad (3c)$$

$$B_R = k_R \sin(\mu_R) + j2\pi\tau f_{R_{\max}} \sin(\gamma_R) \quad (3d)$$

where τ is the time separation, $(\cdot)^*$ denotes the complex conjugate operation, and $\mathbf{E}[\cdot]$ is the statistical expectation operator.

3. NEW SIMULATION MODELS

In this section, based on the reference model introduced in Section 2, we propose the corresponding deterministic and stochastic SoS based simulation models.

3.1. New deterministic simulation model

Before proposing a new deterministic simulation model, which needs only one simulation trial to obtain the desired statistical properties, we would like to first introduce the ‘double-ring’ concept [18] to model non-isotropic scattering M2M scenarios. In such a case, the ‘double-ring’ model defines two rings of effective scatterers, one around the Tx and the other around the Rx, as shown in Figure 1.

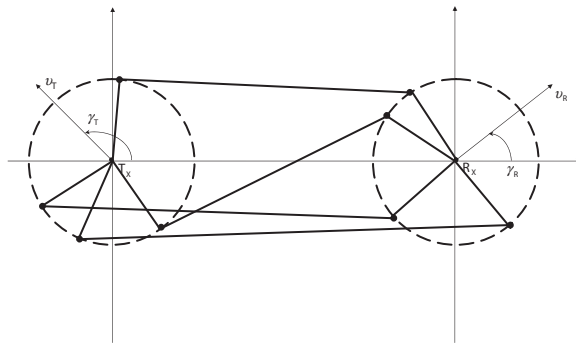


Figure 1. Mobile-to-mobile scattering environment.

To model non-isotropic scattering environments, the effective scatterers are assumed to be non-uniformly distributed. The Tx and Rx move with speeds v_T and v_R in directions determined by the angles of motion γ_T and γ_R , respectively. Based on the ‘double-ring’ model, we can then design a new deterministic simulation model as

$$\tilde{h}(t) = \tilde{h}_i(t) + j\tilde{h}_q(t) \quad (4)$$

$$\begin{aligned} \tilde{h}_i(t) &= \frac{1}{\sqrt{N_i M_i}} \sum_{n_i, m_i=1}^{N_i, M_i} \cos \left[\tilde{\psi}_{n_i m_i} \right. \\ &\quad \left. + 2\pi f_{T_{\max}} t \cos(\tilde{\phi}_T^{m_i} - \gamma_T) \right. \\ &\quad \left. + 2\pi f_{R_{\max}} t \cos(\tilde{\phi}_R^{n_i} - \gamma_R) \right] \end{aligned} \quad (5)$$

$$\begin{aligned} \tilde{h}_q(t) &= \frac{1}{\sqrt{N_q M_q}} \sum_{n_q, m_q=1}^{N_q, M_q} \sin \left[\tilde{\psi}_{n_q m_q} \right. \\ &\quad \left. + 2\pi f_{T_{\max}} t \cos(\tilde{\phi}_T^{m_q} - \gamma_T) \right. \\ &\quad \left. + 2\pi f_{R_{\max}} t \cos(\tilde{\phi}_R^{n_q} - \gamma_R) \right] \end{aligned} \quad (6)$$

where $\tilde{h}_i(t)$ and $\tilde{h}_q(t)$ are in-phase and quadrature components of the complex fading envelope $\tilde{h}(t)$, respectively, $N_{i/q}$ is the number of effective scatterers located on the ring around the Rx, $M_{i/q}$ is the number of effective scatterers located on the ring around the Tx, the AoA $\tilde{\phi}_R^{n_{i/q}}$ and the AoD $\tilde{\phi}_T^{m_{i/q}}$ are discrete realizations of the random variables ϕ_R and ϕ_T , respectively, the phases $\tilde{\psi}_{n_{i/q} m_{i/q}}$ are the single outcomes of the random phases ψ_n in Equation (1). It is assumed that $\tilde{\phi}_R^{n_{i/q}}$, $\tilde{\phi}_T^{m_{i/q}}$, and $\tilde{\psi}_{n_{i/q} m_{i/q}}$ are mutually independent. Note that the AoA $\tilde{\phi}_R^{(n_{i/q})}$ and the AoD $\tilde{\phi}_T^{(m_{i/q})}$ remain constant for different simulation trials due to the deterministic nature of the proposed simulation model. It is worth stressing that the single summation in the reference model (1) is replaced by a double summation due to the double reflection incorporated by the ‘double-ring’ model. However, the channel essentially remains the same for the following two reasons: (1) the assumption of the independence between the AoA and AoD is used in both the reference model (1) and the deterministic simulation model (4); and (2) for both the reference model (1) and the deterministic simulation model (4), each path will be subject to a different Doppler shift due to the motion of both the Tx and Rx.

From the above proposed deterministic simulation model, it is obvious that the key issue in designing a M2M deterministic simulation model is to find the sets of AoAs $\{\tilde{\phi}_R^{n_{i/q}}\}_{n_{i/q}=1}^{N_{i/q}}$ and AoDs $\{\tilde{\phi}_T^{m_{i/q}}\}_{m_{i/q}=1}^{M_{i/q}}$ that make the simulation model reproduce the desired statistical properties of the reference model as faithfully as possible with reasonable complexity, i.e., with a finite number of $N_{i/q}$ and $M_{i/q}$. Under the condition of non-isotropic scattering environments, the PDFs of the AoA ϕ_R and AoD

ϕ_T should be used to design the sets of AoAs $\{\tilde{\phi}_R^{n_{i/q}}\}_{n_{i/q}=1}^{N_{i/q}}$ and AoDs $\{\tilde{\phi}_T^{m_{i/q}}\}_{m_{i/q}=1}^{M_{i/q}}$ that guarantee the uniqueness of the sine and cosine functions related to the AoA $\phi_R^{(n)}$ and AoD $\phi_T^{(m)}$ in the reference model (1). This means that the design of the sets of AoAs and AoDs for the reference model $h(t)$ in Equation (1) should meet the following two conditions:

- (1) $\cos(\tilde{\phi}_R^{n_{i/q}} - \gamma_R) \neq \cos(\tilde{\phi}_R^{n'_{i/q}} - \gamma_R)$, $n_{i/q} \neq n'_{i/q}$; and (2) $\cos(\tilde{\phi}_T^{m_{i/q}} - \gamma_T) \neq \cos(\tilde{\phi}_T^{m'_{i/q}} - \gamma_T)$, $m_{i/q} \neq m'_{i/q}$.

Considering the non-isotropic scattering M2M environments, we now design the sets of AoAs and AoDs of our deterministic simulation model. Via extensive investigation of the PDFs of the AoA ϕ_R and AoD ϕ_T , we find that unlike isotropic scattering M2M environments [18], it is difficult to obtain sets of AoAs and AoDs that meet the two conditions for any non-isotropic scattering M2M environments. Therefore, we divide the non-isotropic scattering M2M environment into the following three categories in terms of the mean AoA μ_R and mean AoD μ_T (i.e., the PDFs of the AoA and AoD), and the angles of motion γ_R and γ_T and then design the sets of AoAs and AoDs separately for these three cases: (1) *Case I*: the main transmitted and received powers come from the same direction as or opposite direction to the movements of the Tx and Rx, respectively, i.e., $|\mu_T - \gamma_T| = |\mu_R - \gamma_R| = 0^\circ$ or π ; (2) *Case II*: the main transmitted and received powers come from the directions that are perpendicular to those of the movements of the Tx and Rx, respectively, i.e., $|\mu_T - \gamma_T| = |\mu_R - \gamma_R| = 90^\circ$; and (3) *Case III*: different from *Cases I* and *II*.

For *Case I*, the in-phase component $h_i(t)$ and quadrature component $h_q(t)$ of the reference model $h(t)$ in Equation (1) are correlated. Therefore, to meet this correlation, we set $N_i = N_q = N$ and $M_i = M_q = M$ and thus the AoA $\tilde{\phi}_R^{n_{i/q}}$ and AoD $\tilde{\phi}_T^{m_{i/q}}$ can be replaced by the $\tilde{\phi}_R^n$ and $\tilde{\phi}_T^m$, respectively. Inspired by the modified method of equal area (MMEA) proposed in Reference [25] for non-isotropic scattering F2M channels, we design the AoA and AOD of our model as

$$\frac{n-1/4}{N} = \int_{\tilde{\phi}_R^{n-1}}^{\tilde{\phi}_R^n} f(\tilde{\phi}_R^n) d\tilde{\phi}_R^n, \quad \tilde{\phi}_R^n \in [-\pi, \pi]$$

$$n = 1, 2, \dots, N \quad (7a)$$

$$\frac{m-1/4}{M} = \int_{\tilde{\phi}_T^{m-1}}^{\tilde{\phi}_T^m} f(\tilde{\phi}_T^m) d\tilde{\phi}_T^m, \quad \tilde{\phi}_T^m \in [-\pi, \pi]$$

$$m = 1, 2, \dots, M \quad (7b)$$

where $\tilde{\phi}_R^0 = -\pi$ and $\tilde{\phi}_T^0 = -\pi$, $f(\tilde{\phi}_R^n)$ and $f(\tilde{\phi}_T^m)$ denote the PDFs of the AoA $\tilde{\phi}_R^n$ and the AoD $\tilde{\phi}_T^m$, respectively. The cumulative distribution functions (CDFs) of the AoA $\tilde{\phi}_R$ and the AoD $\tilde{\phi}_T$ are defined as $F_R(x) = \int_{-\infty}^x f(\tilde{\phi}_R^n) d\tilde{\phi}_R^n$ and $F_T(x) = \int_{-\infty}^x f(\tilde{\phi}_T^m) d\tilde{\phi}_T^m$, respectively. If the inverse functions $F_R^{-1}(\cdot)$ of $F_R(\cdot)$ and $F_T^{-1}(\cdot)$ of $F_T(\cdot)$ exist, (7a) and (7b)

become

$$\tilde{\phi}_R^n = F_R^{-1}\left(\frac{n-1/4}{N}\right) \quad (8a)$$

$$\tilde{\phi}_T^m = F_T^{-1}\left(\frac{m-1/4}{M}\right) \quad (8b)$$

Note that the value of 1/4 used in Equations (8a) and (8b) guarantees that the designed sets of AoAs and AoDs can meet the aforementioned two conditions ($\tilde{\phi}_R^n \neq -\tilde{\phi}_R^{n'} + 2\gamma_R$, $n \neq n'$ and $\tilde{\phi}_T^m \neq -\tilde{\phi}_T^{m'} + 2\gamma_T$, $m \neq m'$) for *Case I*. The proof of the above statement is omitted here since one can easily prove it by following the procedure provided in Reference [25]. The performance of this design will be validated in Section 4.

Under the condition of *Case II*, the cross-correlation between the in-phase component $h_i(t)$ and quadrature component $h_q(t)$ of the complex fading envelope $h(t)$ in Equation (1) is equal to zero. Therefore, by setting $N_i \neq N_q$ and $M_i \neq M_q$ in this case, we can directly use the expression of our simulation model itself to guarantee the aforementioned cross-correlation is equal to zero rather than through the design of the AoAs and AoDs. This makes for a more efficient use of the number of harmonic functions and thus results in better performance of the model. Following the similar parameter computation method of *Case I*, we design the AoA and AoD of our model as

$$\tilde{\phi}_R^{n_{i/q}} = F_R^{-1}\left(\frac{n_{i/q}-1/2}{N_{i/q}}\right), \quad \tilde{\phi}_R^{n_{i/q}} \in [-\pi, \pi]$$

$$n_{i/q} = 1, 2, \dots, N_{i/q} \quad (9a)$$

$$\tilde{\phi}_T^{m_{i/q}} = F_T^{-1}\left(\frac{m_{i/q}-1/2}{M_{i/q}}\right), \quad \tilde{\phi}_T^{m_{i/q}} \in [-\pi, \pi]$$

$$m_{i/q} = 1, 2, \dots, M_{i/q} \quad (9b)$$

Note that the value of 1/2 is applied in Equations (9a) and (9b) instead of the value of 1/4 in Equations (8a) and (8b). The reason is that unlike *Case I*, for *Case II* it is difficult to design sets of AoAs and AoDs that meet the two conditions. Although it is difficult to find one value that can guarantee the designed sets of AoAs and AoDs have the best approximation to the two conditions. Based on simulations and motivated by the modified method of exact Doppler spread (MEDS) in Equations (37) and (38) in Reference [18] for the simulation of isotropic scattering M2M channels, we found that with the value of 1/2, the proposed simulation model presents better performance than the one with other values, e.g., 1/4. The performance of this design will be validated in Section 4.

For *Case III*, since the in-phase and quadrature components of the reference model $h(t)$ in Equation (1) are correlated (similarly to *Case I*) we set $N_i = N_q = N$ and $M_i = M_q = M$ as well and thus the AoA $\tilde{\phi}_R^{n_{i/q}}$ and AoD $\tilde{\phi}_T^{m_{i/q}}$ can be replaced by the $\tilde{\phi}_R^n$ and $\tilde{\phi}_T^m$, respectively.

Following the similar parameter computation method of *Case I*, we design the AoA and AoD of our model as

$$\tilde{\phi}_R^n = F_R^{-1} \left(\frac{n-1/2}{N} \right), \quad \tilde{\phi}_R^n \in [-\pi, \pi]$$

$$n = 1, 2, \dots, N \quad (10a)$$

$$\tilde{\phi}_T^m = F_T^{-1} \left(\frac{m-1/2}{M} \right), \quad \tilde{\phi}_T^m \in [-\pi, \pi]$$

$$m = 1, 2, \dots, M \quad (10b)$$

Note that the value of 1/2 is used in Equations (10a) and (10b) due to the same reason as *Case I*.

The correlation properties of the proposed deterministic simulation model must be analyzed by using time average rather than statistical average. The time-average ACF of the proposed simulation model $\tilde{h}(t)$ is defined as

$$\tilde{\rho}_{\tilde{h}\tilde{h}}(\tau) = \langle \tilde{h}(t)\tilde{h}^*(t-\tau) \rangle \quad (11)$$

where $\langle \cdot \rangle$ denotes the time average operator. Substituting Equation (4) into Equation (11), we have

$$\tilde{\rho}_{\tilde{h}\tilde{h}}(\tau) = 2\tilde{\rho}_{\tilde{h}_i\tilde{h}_i}(\tau) - 2j\tilde{\rho}_{\tilde{h}_i\tilde{h}_q}(\tau) \quad (12)$$

where

$$\tilde{\rho}_{\tilde{h}_i\tilde{h}_i}(\tau) = \frac{1}{2N_iM_i} \sum_{n_i, m_i=1}^{N_i, M_i} \cos [2\pi f_{T_{\max}} \tau \cos(\tilde{\phi}_T^{m_i} - \gamma_T) + 2\pi f_{R_{\max}} \tau \cos(\tilde{\phi}_R^{n_i} - \gamma_R)] \quad (13a)$$

$$\tilde{\rho}_{\tilde{h}_i\tilde{h}_q}(\tau) = \begin{cases} -\frac{1}{2NM} \sum_{n, m=1}^{N, M} \sin [2\pi f_{T_{\max}} \tau \cos(\tilde{\phi}_T^m - \gamma_T) + 2\pi f_{R_{\max}} \tau \cos(\tilde{\phi}_R^n - \gamma_R)] & N_i = N_q = N \text{ and } M_i = M_q \\ 0, & \text{otherwise} \end{cases} \quad (13b)$$

In Appendix A, we give a brief outline of the derivations of Equations (13a) and (13b). From Equation (13b), and based on the corresponding derivation in Appendix A, it is clear that by setting $N_i \neq N_q$ and $M_i \neq M_q$, the cross-correlation between the in-phase component $\tilde{h}_i(t)$ and quadrature component $\tilde{h}_q(t)$ of the proposed simulation model $\tilde{h}(t)$ is equal to zero no matter how the sets of AoAs and AoDs are designed. When N (N_i) and M (M_i) tend to infinity, it is straightforward that the time-average ACF in Equation (12) matches the ensemble average ACF in Equation (2). This allows us to conclude that for $\{N(N_i), M(M_i)\} \rightarrow \infty$, our simulation model can represent the correlation properties of the reference model.

3.2. New stochastic simulation model

Our deterministic model can be further modified to a stochastic simulation model by allowing both the phases

and frequencies to be random variables. Unlike the deterministic model, the properties of the stochastic model vary for each simulation trial, but will converge to the desired ones when averaged over a sufficient number of simulation trials. A hat is used to distinguish this model from the deterministic one, thus

$$\hat{h}(t) = \hat{h}_i(t) + j\hat{h}_q(t) \quad (14)$$

$$\hat{h}_i(t) = \frac{1}{\sqrt{N_iM_i}} \sum_{n_i, m_i=1}^{N_i, M_i} \cos [\hat{\psi}_{n_i m_i} + 2\pi f_{T_{\max}} t \cos(\hat{\phi}_T^{m_i} - \gamma_T) + 2\pi f_{R_{\max}} t \cos(\hat{\phi}_R^{n_i} - \gamma_R)] \quad (15)$$

$$\hat{h}_q(t) = \frac{1}{\sqrt{N_qM_q}} \sum_{n_q, m_q=1}^{N_q, M_q} \sin [\hat{\psi}_{n_q m_q} + 2\pi f_{T_{\max}} t \cos(\hat{\phi}_T^{m_q} - \gamma_T) + 2\pi f_{R_{\max}} t \cos(\hat{\phi}_R^{n_q} - \gamma_R)] \quad (16)$$

where $\hat{h}_i(t)$ and $\hat{h}_q(t)$ are in-phase and quadrature components of complex fading envelope $\hat{h}(t)$, respectively, $\hat{\phi}_R^{n_i/q}$ and $\hat{\phi}_T^{m_i/q}$ denote the AoA and AoD of our stochastic simulation model, respectively, and the phases $\hat{\psi}_{n_i/q m_i/q}$ are random variables uniformly distributed on the interval $[-\pi, \pi]$. Parameters $\hat{\phi}_R^{n_i/q}$, $\hat{\phi}_T^{m_i/q}$, and $\hat{\psi}_{n_i/q m_i/q}$ are independent of each

other. Note that unlike the AoA and AoD in a deterministic simulation model, the AoA $\hat{\phi}_R^{n_i/q}$ and AoD $\hat{\phi}_T^{m_i/q}$ are random variables and thus vary for different simulation trials. The fundamental issue for the design of the sets of AoAs $\{\hat{\phi}_R^{n_i/q}\}_{n_i/q=1}^{N_i/q}$ and AoDs $\{\hat{\phi}_T^{m_i/q}\}_{m_i/q=1}^{M_i/q}$ is how to incorporate a random term into the AoA and AoD. In this paper, to deal with this fundamental issue, we apply the method proposed in Reference [12] for the simulation of isotropic scattering F2M channels. Based on the comparative analysis in Reference [26], we can conclude that the smaller (but sufficient) range on which the AoA $\hat{\phi}_R^{n_i/q}$ and AoD $\hat{\phi}_T^{m_i/q}$ are designed, the better performance the stochastic model that will be obtained. Based on the extensive investigation of the PDFs of the AoA ϕ_R and AoD ϕ_T , we find that unlike isotropic scattering M2M environments [18], the appropriate range on which the AoA and AoD are designed varies for different non-isotropic scattering M2M environments. Therefore, similarly to our deterministic model, we design the sets of AoAs and AoDs of our stochastic model

separately for the following three cases: (1) *Case I*: the main transmitted and received powers come from the same direction as the movements of the Tx and Rx that is along x axis, i.e., $\mu_T = \gamma_T = \mu_R = \gamma_R = 0^\circ$ or π ; (2) *Case II*: the main transmitted and received powers come from the directions that are perpendicular to those of the movements of the Tx and Rx, respectively, i.e., $|\mu_T - \gamma_T| = |\mu_R - \gamma_R| = 90^\circ$; and (3) *Case III*: different from *Cases I* and *II*.

For *Case I*, due to the same reason as the design of our deterministic model for *Case I* we have $N_i = N_q = N$ and $M_i = M_q = M$ and thus the AoA $\hat{\phi}_R^{n_{i/q}}$ and AoD $\hat{\phi}_T^{m_{i/q}}$ can be replaced by the $\hat{\phi}_R^n$ and $\hat{\phi}_T^m$, respectively. In this case, we found that the PDFs of the AoA and AoD are symmetric with respect to the origin. Therefore, the appropriate ranges for the design of both AoA and AoD are from 0 to π because the rest of the range is redundant (i.e., the range $[-\pi, 0)$ provides us with the same information as $[0, \pi)$). Inspired by the method in Reference [12] for isotropic scattering F2M channels, we design the AoA and AoD of our model as

$$\hat{\phi}_R^n = F_R^{-1} \left(\frac{n - 1/2 + \theta_R}{N} \right), \quad \hat{\phi}_R^n \in [0, \pi)$$

$$n = 1, 2, \dots, N \tag{17a}$$

$$\hat{\phi}_T^m = F_T^{-1} \left(\frac{m - 1/2 + \theta_T}{M} \right), \quad \hat{\phi}_T^m \in [0, \pi)$$

$$m = 1, 2, \dots, M \tag{17b}$$

where θ_R and θ_T are random variables uniformly distributed on the interval $[-1/2, 1/2)$ and are independent to each other. It is worth stressing that the interval $[-1/2, 1/2)$ and the constant value of $1/2$ are chosen to guarantee that the design of the AoA and AoD is based on the desired range (here is $[0, \pi)$). This indicates that any interval and the corresponding constant value can be chosen only if they can fulfill the aforementioned guarantee (e.g., the interval is $[0, 1)$ and constant value is 1). Note that the introduction of the random terms θ_R and θ_T in the AoA $\hat{\phi}_R^n$ and AoD $\hat{\phi}_T^m$, respectively, leads to the AoA and AoD being random variables and thus varying for different simulation trials. $\tilde{\phi}_R^{n_{i/q}}$ and AoD $\tilde{\phi}_T^{m_{i/q}}$ of our deterministic simulation model, which are constant for different simulation trials.

For *Case II*, analogous to our deterministic model, we impose $N_i \neq N_q$ and $M_i \neq M_q$ in our stochastic model to guarantee the cross-correlation between the in-phase component $\hat{h}_i(t)$ and quadrature component $\hat{h}_q(t)$ of the proposed stochastic model $\hat{h}(t)$ for one simulation trial is equal to zero. In this case, since the PDFs of the AoA and AoD are asymmetric with respect to the origin, the full range (i.e., from $-\pi$ to π) is needed for the design of the AoA and AoD. Therefore, we can express the AoA and AoD as

$$\hat{\phi}_R^{n_{i/q}} = F_R^{-1} \left(\frac{n_{i/q} - 1/2 + \theta_R}{N_{i/q}} \right), \quad \hat{\phi}_R^{n_{i/q}} \in [0, \pi)$$

$$n_{i/q} = 1, 2, \dots, N_{i/q} \tag{18a}$$

$$\hat{\phi}_T^{m_{i/q}} = F_T^{-1} \left(\frac{m_{i/q} - 1/2 + \theta_T}{M_{i/q}} \right), \quad \hat{\phi}_T^{m_{i/q}} \in [-\pi, \pi)$$

$$m_{i/q} = 1, 2, \dots, M_{i/q} \tag{18b}$$

For *Case III*, due to the same reason as *Case I* we have $N_i = N_q = N$ and $M_i = M_q = M$ and thus the AoA $\hat{\phi}_R^{n_{i/q}}$ and AoD $\hat{\phi}_T^{m_{i/q}}$ can be replaced by the $\hat{\phi}_R^n$ and $\hat{\phi}_T^m$, respectively. In this case, analogous to *Case II*, we know that the full range (i.e., from $-\pi$ to π) is necessary for the design of the AoA and AoD. Therefore, the AoA and AoD can be designed as

$$\hat{\phi}_R^n = F_R^{-1} \left(\frac{n - 1/2 + \theta_R}{N} \right), \quad \hat{\phi}_R^n \in [-\pi, \pi)$$

$$n = 1, 2, \dots, N \tag{19a}$$

$$\hat{\phi}_T^m = F_T^{-1} \left(\frac{m - 1/2 + \theta_T}{M} \right), \quad \hat{\phi}_T^m \in [-\pi, \pi)$$

$$m = 1, 2, \dots, M \tag{19b}$$

Unlike our deterministic simulation model, the time ACF of our stochastic simulation model should be computed according to $\hat{\rho}_{\hat{h}\hat{h}}(\tau) = \mathbf{E}[\hat{h}(t)\hat{h}^*(t - \tau)]$. It can be shown that our stochastic model exhibits correlation properties of the reference model irrespective of the values of $N_{i/q}$ and $M_{i/q}$, i.e., for any $N_{i/q}$ and $M_{i/q}$. Appendix B outlines the derivation of the ACF $\hat{\rho}_{\hat{h}\hat{h}}(\tau)$ for the model $\hat{h}(t)$.

It is worth noting that the proposed stochastic model shows better performance and has lower complexity than the ARA model [22]. Since in Reference [22] the authors did not give the detailed explanation on how to generate the AoAs and AoDs for their model by using the ARA, it is impossible to reproduce this model. Therefore, to validate the above statement, in Figure 2 we compare the ACF of the real part of the ARA model obtained from Figure 5 in Reference [22] with the one of our model. For a fair comparison, the same parameters as those used in Figure 5 in

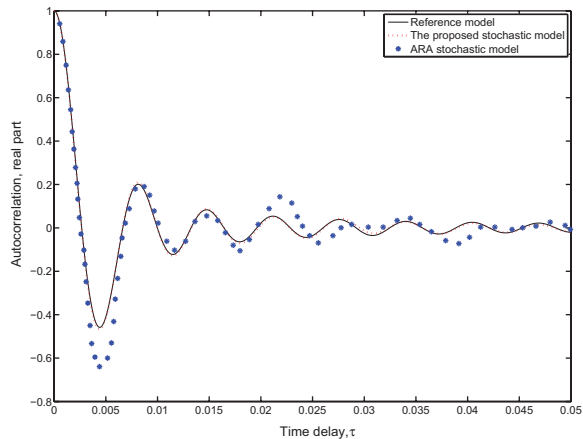


Figure 2. Comparison between the proposed stochastic model and the ARA stochastic model proposed in Reference [22].

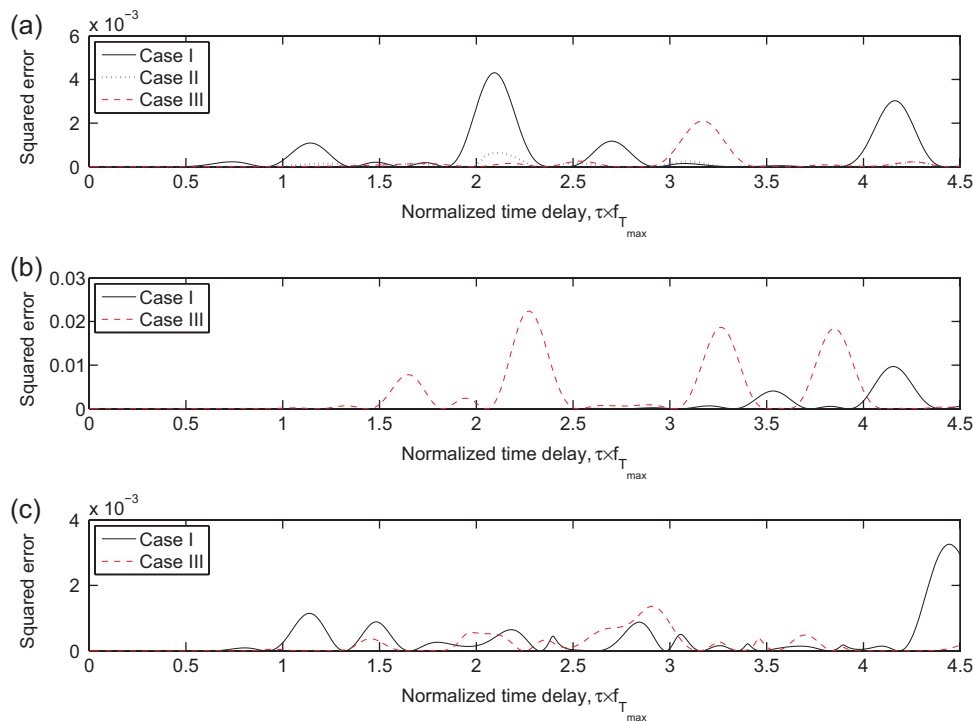


Figure 3. Squared error in the CF of the proposed deterministic simulation model with $k_T = k_R = 1$ for different non-isotropic scattering M2M Rayleigh fading channels: (a) $\mu_T = \mu_R = 110^\circ$ and $\gamma_T = \gamma_R = 20^\circ$; (b) $\mu_T = \mu_R = \gamma_T = \gamma_R = 0^\circ$; (c) $\mu_T = 30^\circ$, $\mu_R = 160^\circ$, $\gamma_T = 10^\circ$, and $\gamma_R = 20^\circ$.

Reference [22] are used, namely $f_{T_{max}} = 100$ Hz, $f_{R_{max}} = 50$ Hz, $\mu_T = \pi/4$, $\mu_R = -\pi/4$, $k_T = k_R = 3$, $\gamma_T = \gamma_R = 0^\circ$, and the number of simulation trials $N_{stat} = 10$. Note that the number of harmonic functions used in the ARA model is $P = 144$, while in our model is $N_i = M_i = 10$. From Figure 2, it is obvious that our model outperforms the ARA model with even smaller number of harmonic functions, i.e., $N_i \times M_i = 100 < P$.

4. NUMERICAL RESULTS AND ANALYSIS

In this section, we first validate the newly proposed deterministic model by using the squared error between the correlation properties of the simulation model and those of the reference model. Then the validation of the proposed stochastic simulation model is performed by utilizing the difference in the time average properties of a single simulation trial for the stochastic model from the desired ensemble average properties. Furthermore, the performance evaluation of the proposed models is carried out by comparing the correlation properties of the proposed simulation models with those of the reference model. Unless otherwise specified, all the results presented here are obtained using $f_{T_{max}} = f_{R_{max}} = 100$ Hz, $N_i = M_i = N_q = M_q = 20$ for Cases I, III and $N_i = M_i = 20$, $N_q = M_q = 21$ for Case II of the deterministic model, $N_i = M_i = N_q = M_q = 10$

for Cases I, III and $N_i = M_i = 10$, $N_q = M_q = 11$ for Case II of the stochastic model, and the normalized sampling period $f_{T_{max}} T_s = 0.005$ (T_s is the sampling period).

To validate our deterministic model, in Figure 3 we compare the difference in the ACF $\tilde{\rho}_{hh}(\tau)$ from the desired $\rho_{hh}(\tau)$ using the squared error $|\tilde{\rho}_{hh}(\tau) - \rho_{hh}(\tau)|^2$ for different non-isotropic M2M scenarios. Similarly, to validate our stochastic model, Figure 4 compares the difference in the time averaged ACF of a single simulation trial $\check{\rho}_{hh}(\tau)$ from the desired ACF $\rho_{hh}(\tau)$ as $\mathbf{E}[|\check{\rho}_{hh}(\tau) - \rho_{hh}(\tau)|^2]$ for different non-isotropic M2M scenarios. As pointed out in Reference [26], this provides a measure of the utility of the stochastic model in simulating the desired channel waveform using a finite harmonic functions $N_{i/q}$ and $M_{i/q}$. The results in Figure 4 are obtained by averaging over 10^4 simulation trials for each value of time delay τ . Note that for the sake of the readability of figures, the difference of our models for Case II is only shown in Figures 3(a) and 4(a) since this is extremely large for other cases. In addition, for longer time delays, the deviation of our simulation model for all cases become extremely large due to the insufficient number of harmonic functions. To maintain readability of the figures, we have removed the longer time delays and only presented shorter time delays, which is typically of interest for most communication systems [18]. From Figures 3 and 4, it is clear that due to the impact of non-isotropic scattering, no one parameter computation method in our models consistently outperforms others for all non-isotropic M2M scenarios. This,

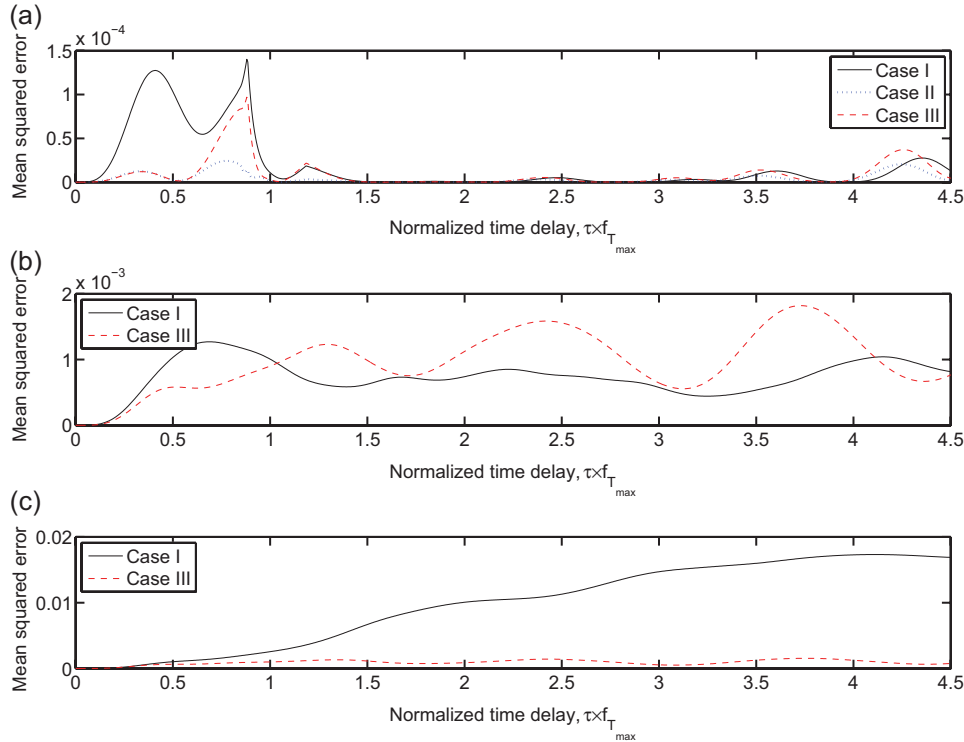


Figure 4. Mean squared error in the CF of the proposed stochastic simulation model with $k_T = k_R = 5$ for different non-isotropic scattering M2M Rayleigh fading channels: (a) $\mu_T = \mu_R = 110^\circ$ and $\gamma_T = \gamma_R = 20^\circ$; (b) $\mu_T = \mu_R = \gamma_T = \gamma_R = 0^\circ$; (c) $\mu_T = 20^\circ$, $\mu_R = 10^\circ$, $\gamma_T = 10^\circ$, and $\gamma_R = 20^\circ$.

hence, validates the utility of our models that include three different sets of model parameters rather than only one.

To evaluate the performance of our simulation models, in Figures 5–7 we give a comparison between the ACF of the reference model and the one of our simulation models for various values of k_T , k_R , μ_T , and μ_R . The results obtained

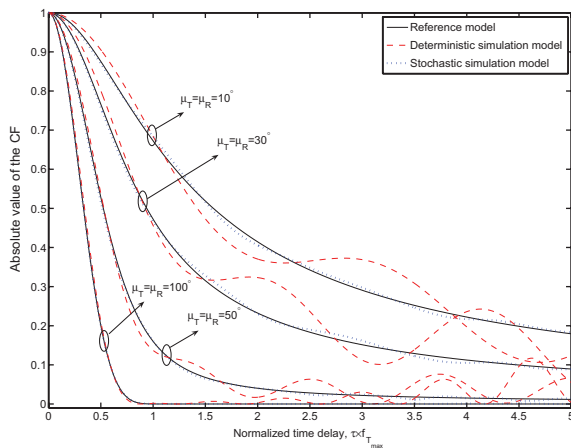


Figure 5. Comparison between the CF of the reference model and the one of the proposed simulation models with $k_T = k_R = 6$ and $\gamma_T = \gamma_R = 10^\circ$ for various values of the mean AoD μ_T and mean AoA μ_R .

for the stochastic model are averaged over $N_{stat} = 10$ simulation trials. It is obvious that the deterministic model provides a fairly good approximation to the ACF of the reference model in a shorter normalized time-delay range, while the stochastic model presents much better approximation even with a smaller number of harmonic functions $N_{i/q}$ and $M_{i/q}$. Compared to our deterministic model, our stochastic model has a higher complexity since it requires several simulation trials to achieve the desired properties. Notice that the quality of the approximation between the ACFs of our deterministic model and the reference model can be improved by increasing the values of $N_{i/q}$ and $M_{i/q}$, while the quality of the approximation between the ACF of our stochastic model and the one of the reference model can be improved by increasing the values of $N_{i/q}$ and $M_{i/q}$, and/or the value of N_{stat} . More interestingly, from Figure 5, we observe that the increase of the values of $|\mu_T - \gamma_T|$ and $|\mu_R - \gamma_R|$ decreases the difficulty of our simulation model in approximating the correlation properties of the reference model. Similarly, Figure 6 shows that the difficulty of our simulation model in approximating the correlation properties of the reference model increases with the increase of the values of k_T and k_R . More importantly, Figures 5–7 show that when the values of $|\mu_T - \gamma_T|$ and $|\mu_R - \gamma_R|$ are small and/or the values of k_T and k_R are large, the proposed deterministic simulation model cannot even approximate the correlation properties of the reference model for short

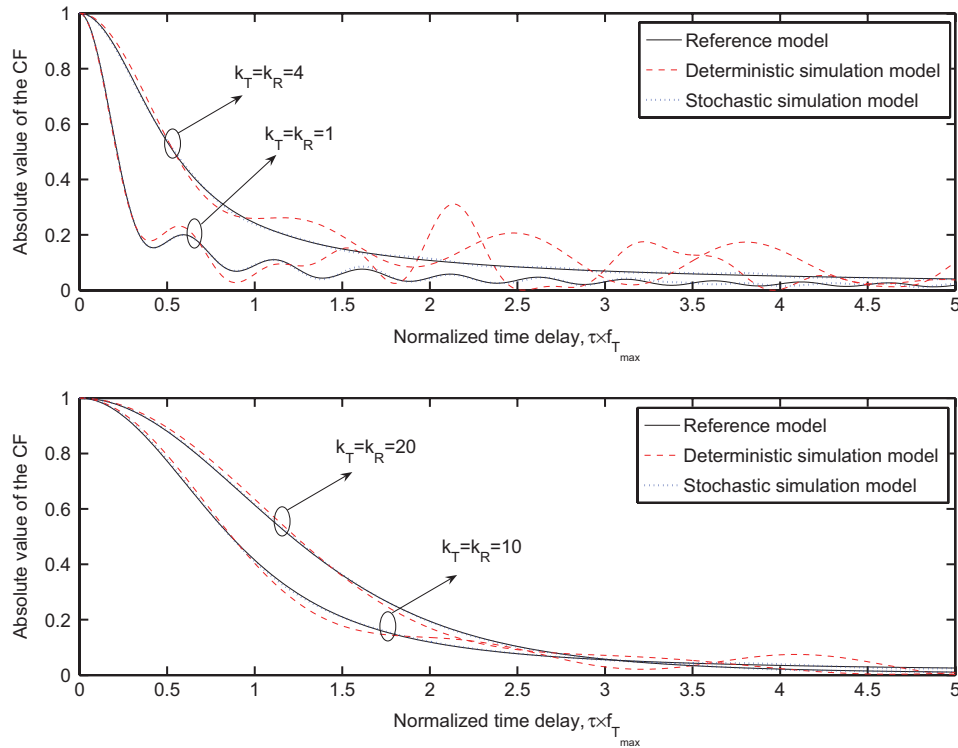


Figure 6. Comparison between the CF of the reference model and the one of the proposed simulation models with $\mu_T = \mu_R = 60^\circ$ and $\gamma_T = \gamma_R = 30^\circ$ for various values of k_T and k_R .

time-delays. In the aforementioned situations, to obtain an acceptable approximation between the correlation properties of our deterministic model and the ones of the reference model, a large number of harmonic functions (here $N_i = M_i = N_q = M_q = 60$ as depicted in Figure 7) is necessary. This allows us to conclude that the stochastic simulation

model is more suitable than the deterministic model for such a non-isotropic scattering M2M scenario where the differences between the angles of motion γ_T and γ_R , and the mean AoA μ_T and AoD μ_R are small (i.e., the value of $|\mu_T - \gamma_T|$ and $|\mu_R - \gamma_R|$ are small) and/or the received powers are more concentrated in one direction (i.e., the value of k_T and k_R are large).

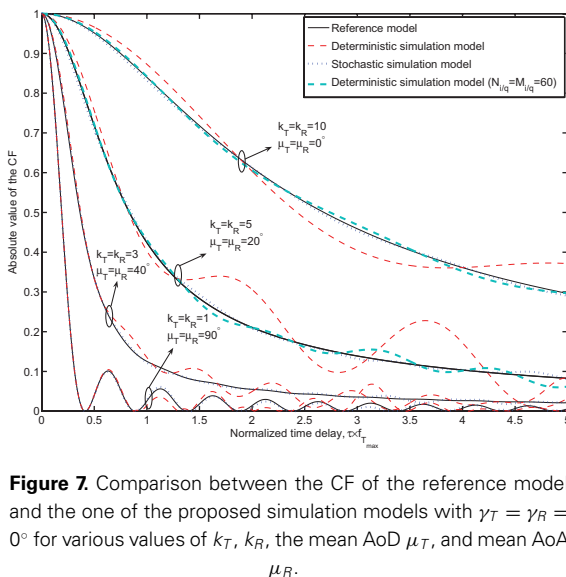


Figure 7. Comparison between the CF of the reference model and the one of the proposed simulation models with $\gamma_T = \gamma_R = 0^\circ$ for various values of k_T , k_R , the mean AoD μ_T , and mean AoA μ_R .

5. CONCLUSIONS

In this paper, based on the ‘double-ring’ concept and the comprehensive analysis of the PDFs of the AoA and AoD, new deterministic and stochastic SoS based simulation models have been proposed for non-isotropic M2M Rayleigh fading channels. The performance of the proposed simulation models has been verified in terms of the CF through the theoretical and simulation results. Results have shown that compared to the proposed deterministic model, the proposed stochastic model provides better approximation of the reference model even with a smaller number of harmonic functions. Moreover, our analysis has revealed that the proposed stochastic model performs better than the ARA stochastic model. Finally, either the proposed deterministic (lower complexity) model or stochastic (higher accuracy) model can be used for simulations of M2M systems.

ACKNOWLEDGMENTS

X. Cheng, C.-X. Wang, and D. I. Laurenson acknowledge the support from the Scottish Funding Council for the Joint Research Institute in Signal and Image Processing between the University of Edinburgh and Heriot-Watt University- which is a part of the Edinburgh Research Partnership in Engineering and Mathematics (ERPem).

The integral of Equation (20) is trivial as the integrand does not contain the variable of integration. Therefore, the expression of $\tilde{\rho}_{\tilde{h}_i, \tilde{h}_q}(\tau)$ in Equation (13a) can be easily obtained from Equation (20).

The derivation of the time-average cross-correlation function $\tilde{\rho}_{\tilde{h}_i, \tilde{h}_q}(\tau)$ between the in-phase component $\tilde{h}_i(t)$ (5) and the quadrature component $\tilde{h}_q(t)$ (6) of the proposed deterministic simulation model is outlined as follows:

$$\begin{aligned} \tilde{\rho}_{\tilde{h}_i, \tilde{h}_q}(\tau) &= \langle \tilde{h}_i(t) \tilde{h}_q(t - \tau) \rangle = \lim_{T \rightarrow \infty} \frac{1}{2T} \int_{-T}^T \tilde{h}_i(t) \tilde{h}_q(t - \tau) dt \\ &= \lim_{T \rightarrow \infty} \frac{1}{2T} \int_{-T}^T \frac{1}{\sqrt{N_i M_i} \sqrt{N_q M_q}} \sum_{n_i, m_i=1}^{N_i, M_i} \sum_{n_q, m_q=1}^{N_q, M_q} \cos [\tilde{\psi}_{n_i m_i} + 2\pi f_{T_{\max}} t \cos(\tilde{\phi}_T^{m_i} - \gamma_T) \\ &\quad + 2\pi f_{R_{\max}} t \cos(\tilde{\phi}_R^{n_i} - \gamma_R)] \sin [\tilde{\psi}_{n_q m_q} + 2\pi f_{T_{\max}} (t - \tau) \cos(\tilde{\phi}_T^{m_q} - \gamma_T) \\ &\quad + 2\pi f_{R_{\max}} (t - \tau) \cos(\tilde{\phi}_R^{n_q} - \gamma_R)] dt \\ &= \begin{cases} - \lim_{T \rightarrow \infty} \frac{1}{2T} \int_{-T}^T \frac{1}{2NM} \sum_{n, m=1}^{N, M} \sin [2\pi f_{T_{\max}} \tau \cos(\tilde{\phi}_T^m - \gamma_T) & N_i = N_q = N \text{ and } M_i = M_q \\ \quad + 2\pi f_{R_{\max}} \tau \cos(\tilde{\phi}_R^n - \gamma_R)] dt, & = M \quad (\text{Cases I and III}) \\ 0 & N_i \neq N_q \text{ and } M_i \neq M_q \text{ (Case II)} \end{cases} \end{aligned} \tag{21}$$

Appendix A: Derivation of Equation (13a) and (13b)

In this appendix, we first derive the time-average ACF $\tilde{\rho}_{\tilde{h}_i, \tilde{h}_i}(\tau)$ of the in-phase component $\tilde{h}_i(t)$ (5) of the proposed deterministic simulation model

$$\begin{aligned} \tilde{\rho}_{\tilde{h}_i, \tilde{h}_i}(\tau) &= \langle \tilde{h}_i(t) \tilde{h}_i(t - \tau) \rangle = \lim_{T \rightarrow \infty} \frac{1}{2T} \int_{-T}^T \tilde{h}_i(t) \tilde{h}_i(t - \tau) dt \\ &= \lim_{T \rightarrow \infty} \frac{1}{2T} \int_{-T}^T \frac{1}{N_i M_i} \sum_{n_i, m_i=1}^{N_i, M_i} \sum_{n'_i, m'_i=1}^{N_i, M_i} \cos [\tilde{\psi}_{n_i m_i} + 2\pi f_{T_{\max}} t \cos(\tilde{\phi}_T^{m_i} - \gamma_T) \\ &\quad + 2\pi f_{R_{\max}} t \cos(\tilde{\phi}_R^{n_i} - \gamma_R)] \cos [\tilde{\psi}_{n'_i m'_i} + 2\pi f_{T_{\max}} (t - \tau) \cos(\tilde{\phi}_T^{m'_i} - \gamma_T) \\ &\quad + 2\pi f_{R_{\max}} (t - \tau) \cos(\tilde{\phi}_R^{n'_i} - \gamma_R)] dt \\ &= \lim_{T \rightarrow \infty} \frac{1}{2T} \int_{-T}^T \frac{1}{N_i M_i} \sum_{n_i, m_i=1}^{N_i, M_i} \cos [\tilde{\psi}_{n_i m_i} + 2\pi f_{T_{\max}} t \cos(\tilde{\phi}_T^{m_i} - \gamma_T) + 2\pi f_{R_{\max}} t \cos(\tilde{\phi}_R^{n_i} - \gamma_R)] \\ &\quad \times \cos [\tilde{\psi}_{n_i m_i} + 2\pi f_{T_{\max}} (t - \tau) \cos(\tilde{\phi}_T^{m_i} - \gamma_T) + 2\pi f_{R_{\max}} (t - \tau) \cos(\tilde{\phi}_R^{n_i} - \gamma_R)] dt \\ &\quad (\text{since } n_i \neq n'_i \text{ and/or } m_i \neq m'_i, \tilde{\rho}_{\tilde{h}_i, \tilde{h}_i}(\tau) = 0) \\ &= \lim_{T \rightarrow \infty} \frac{1}{2T} \int_{-T}^T \frac{1}{2N_i M_i} \sum_{n_i, m_i=1}^{N_i, M_i} \cos [2\pi f_{T_{\max}} \tau \cos(\tilde{\phi}_T^{m_i} - \gamma_T) + 2\pi f_{R_{\max}} \tau \cos(\tilde{\phi}_R^{n_i} - \gamma_R)] dt \end{aligned} \tag{20}$$

where at the third equality of Equation (21), setting $N_i \neq N_q$ and $M_i \neq M_q$ results in the integrand for Case II containing the variable of integration t unlike the integrand for other cases.

Appendix B: Derivation of the CF

$$\hat{\rho}_{\hat{h}\hat{h}}(\tau)$$

In this appendix, we derive the CF $\hat{\rho}_{\hat{h}\hat{h}}(\tau)$ for the stochastic simulation model in Equation (14)

$$\hat{\rho}_{\hat{h}\hat{h}}(\tau) = E [\hat{h}(t) \hat{h}^*(t - \tau)]$$

$$= \left\{ \begin{aligned} & \frac{1}{NM} \sum_{n,m=1}^{N,M} \int_{-\frac{1}{2}}^{\frac{1}{2}} \int_{-\frac{1}{2}}^{\frac{1}{2}} e^{j2\pi\tau \{ f_{T_{\max}} \cos [F^{-1}(\frac{n-1/2+\theta_T}{vM}) - \gamma_T] + f_{R_{\max}} \cos [F^{-1}(\frac{n-1/2+\theta_R}{uN}) - \gamma_R] \}} d\theta_T d\theta_R, \\ & \hspace{15em} N_i = N_q = N \text{ and } M_i = M_q = M \hspace{5em} \text{(Cases I and III)} \\ & \frac{1}{2N_i M_i} \sum_{n_i, m_i=1}^{N_i, M_i} \int_{-\frac{1}{2}}^{\frac{1}{2}} \int_{-\frac{1}{2}}^{\frac{1}{2}} \cos \left\{ 2\pi\tau \left(f_{T_{\max}} \cos \left[F^{-1} \left(\frac{m_i - 1/2 + \theta_T}{M_i} \right) - \gamma_T \right] \right. \right. \\ & \quad \left. \left. + f_{R_{\max}} \cos \left[F^{-1} \left(\frac{n_i - 1/2 + \theta_R}{N_i} \right) - \gamma_R \right] \right) \right\} d\theta_T d\theta_R \\ & + \frac{1}{2N_q M_q} \sum_{n_q, m_q=1}^{N_q, M_q} \int_{-\frac{1}{2}}^{\frac{1}{2}} \int_{-\frac{1}{2}}^{\frac{1}{2}} \cos \left\{ 2\pi\tau \left(f_{T_{\max}} \cos \left[F^{-1} \left(\frac{m_q - 1/2 + \theta_T}{M_q} \right) - \gamma_T \right] \right. \right. \\ & \quad \left. \left. + f_{R_{\max}} \cos \left[F^{-1} \left(\frac{n_q - 1/2 + \theta_R}{N_q} \right) - \gamma_R \right] \right) \right\} d\theta_T d\theta_R, \hspace{5em} \text{(Case II)} \end{aligned} \right.$$

$$= \left\{ \begin{aligned} & \frac{NM}{NM} \sum_{n,m=1}^{N,M} \int_{F^{-1}(\frac{n-1}{uN})}^{F^{-1}(\frac{n}{uN})} \int_{F^{-1}(\frac{m-1}{vM})}^{F^{-1}(\frac{m}{vM})} e^{j2\pi\tau [f_{T_{\max}} \cos(\beta_T^m - \gamma_T) + f_{R_{\max}} \cos(\beta_R^n - \gamma_R)]} \frac{e^{k_T \cos(\beta_T^m - \mu_T) + k_R \cos(\beta_R^n - \mu_R)}}{4\pi^2 I_0(k_T) I_0(k_R)} d\beta_T^m d\beta_R^n \\ & \hspace{15em} N_i = N_q = N \text{ and } M_i = M_q = M \hspace{5em} \text{(Cases I and III)} \\ & \frac{N_i M_i}{2N_i M_i} \sum_{n_i, m_i=1}^{N_i, M_i} \int_{F^{-1}(\frac{n_i-1}{N_i})}^{F^{-1}(\frac{n_i}{N_i})} \int_{F^{-1}(\frac{m_i-1}{M_i})}^{F^{-1}(\frac{m_i}{M_i})} \cos \left\{ 2\pi\tau [f_{T_{\max}} \cos(\beta_T^{m_i} - \gamma_T) + f_{R_{\max}} \cos(\beta_R^{n_i} - \gamma_R)] \right\} \\ & \quad \times \frac{e^{k_T \cos(\beta_T^{m_i} - \mu_T) + k_R \cos(\beta_R^{n_i} - \mu_R)}}{4\pi^2 I_0(k_T) I_0(k_R)} d\beta_T^{m_i} d\beta_R^{n_i} + \frac{N_q M_q}{2N_q M_q} \sum_{n_q, m_q=1}^{N_q, M_q} \int_{F^{-1}(\frac{n_q-1}{N_q})}^{F^{-1}(\frac{n_q}{N_q})} \int_{F^{-1}(\frac{m_q-1}{M_q})}^{F^{-1}(\frac{m_q}{M_q})} \cos \left\{ 2\pi\tau \left[f_{T_{\max}} \right. \right. \\ & \quad \left. \left. \times \cos(\beta_T^{m_q} - \gamma_T) + f_{R_{\max}} \cos(\beta_R^{n_q} - \gamma_R) \right] \right\} \frac{e^{k_T \cos(\beta_T^{m_q} - \mu_T) + k_R \cos(\beta_R^{n_q} - \mu_R)}}{4\pi^2 I_0(k_T) I_0(k_R)} d\beta_T^{m_q} d\beta_R^{n_q} \hspace{5em} \text{(Case II)} \end{aligned} \right.$$

$$\begin{aligned}
 & \left\{ \begin{aligned}
 & \frac{1}{2\pi^2 I_0(k_T) I_0(k_R)} \int_0^\pi \int_0^\pi e^{j2\pi\tau [f_{T\max} \cos(\beta_T - \gamma_T) + f_{R\max} \cos(\beta_R - \gamma_R)]} \\
 & \quad \times e^{k_T \cos(\beta_T^m - \mu_T) + k_R \cos(\beta_R^m - \mu_R)} d\beta_T d\beta_R, \tag{Case I} \\
 & \frac{1}{4\pi^2 I_0(k_T) I_0(k_R)} \int_{-\pi}^\pi \int_{-\pi}^\pi \cos \left\{ 2\pi\tau [f_{T\max} \cos(\beta_T - \gamma_T) + f_{R\max} \cos(\beta_R - \gamma_R)] \right\} \\
 & \quad \times e^{k_T \cos(\beta_T - \mu_T) + k_R \cos(\beta_R - \mu_R)} d\beta_T d\beta_R, \tag{Case II} \\
 & \frac{1}{4\pi^2 I_0(k_T) I_0(k_R)} \int_{-\pi}^\pi \int_{-\pi}^\pi e^{j2\pi\tau [f_{T\max} \cos(\beta_T - \gamma_T) + f_{R\max} \cos(\beta_R - \gamma_R)]} \\
 & \quad \times e^{k_T \cos(\beta_T^m - \mu_T) + k_R \cos(\beta_R^m - \mu_R)} d\beta_T d\beta_R \tag{Case III}
 \end{aligned} \right. \\
 & \tag{22}
 \end{aligned}$$

where at the second equality of Equation (22), the integration variables θ_T and θ_R were replaced by

$$\begin{aligned}
 \beta_T^{m_{i/q}} &= F^{-1} \left(\frac{m_{i/q} - 1/2 + \theta_T}{M_{i/q}} \right), & d\theta_T &= \frac{M_{i/q} e^{k_T \cos(\beta_T^{m_{i/q}} - \mu_T)}}{2\pi I_0(k_T)} d\beta_T^{m_{i/q}}, \\
 \beta_R^{n_{i/q}} &= F^{-1} \left(\frac{n_{i/q} - 1/2 + \theta_R}{N_{i/q}} \right), & d\theta_R &= \frac{N_{i/q} e^{k_R \cos(\beta_R^{n_{i/q}} - \mu_R)}}{2\pi I_0(k_R)} d\beta_R^{n_{i/q}}, \\
 d\beta_R^{n_{i/q}}, & \beta_T^m &= F^{-1} \left(\frac{m - 1/2 + \theta_T}{M} \right), & d\theta_T &= \frac{M e^{k_T \cos(\beta_T^m - \mu_T)}}{2\pi I_0(k_T)} d\beta_T^m, \\
 d\beta_T^m, & \beta_R^n &= F^{-1} \left(\frac{n - 1/2 + \theta_R}{N} \right), & d\theta_R &= \frac{N e^{k_R \cos(\beta_R^n - \mu_R)}}{2\pi I_0(k_R)} d\beta_R^n.
 \end{aligned}$$

The tow single definite integrals in the last equality of (22) can be solved by using the equality $\int_{-\pi}^\pi e^{a \sin c + b \cos c} dc = 2\pi I_0(\sqrt{a^2 + b^2})$ [27]. After some manipulation, the closed-form expression of the CF $\hat{\rho}_{hh}(\tau)$ can be obtained and is the same as $\rho_{hh}(\tau)$ in Equation (2).

REFERENCES

1. Kojima F, Harada H, Fujise M. Inter-vehicle communication network with an autonomous relay access scheme. *Transactions on Communications* 2001; **E83-B**(3): 566–575.
2. Pabst R, Walke BH, Schultz DC, *et al.* Relay-based deployment concepts for wireless and mobile broadband radio. *IEEE Communications Magazine* 2004; **42**(9): 80–89.
3. IEEE P802.11p/D2.01. Standard for wireless local area networks providing wireless communications while in vehicular environment. *Technical Report*, March 2007.
4. Akki AS, Haber F. A statistical model for mobile-to-mobile land communication channel. *IEEE Transactions on Vehicular Technology* 1986; **35**(1): 2–10.
5. Akki AS. Statistical properties of mobile-to-mobile land communication channels. *IEEE Transactions on Vehicular Technology* 1994; **43**(4): 826–831.
6. Zajić AG, Stüber GL. Space-time correlated mobile-to-mobile channels: modelling and simulation. *IEEE Transactions on Vehicular Technology* 2008; **57**(2): 715–726.

7. Zajić AG, Stüber GL, Pratt TG, Nguyen S. Wideband MIMO mobile-to-mobile channels: geometry-based statistical modeling with experimental verification. *IEEE Transactions on Vehicular Technology* 2009; **58**(2): 517–634.
8. Sen I, Matolak DW. Vehicle-vehicle channel models for the 5-GHz band. *IEEE Transactions on Intelligent Transportation Systems* 2008; **9**(2): 235–245.
9. Cheng X, Wang C-X, Laurenson DI, Vasilakos AV. Second order statistics of non-isotropic mobile-to-mobile Ricean fading channels. *Proceedings of IEEE ICC'09*, Dresden, Germany, June 2009.
10. Cheng X, Wang C-X, Laurenson DI, Salous S, Vasilakos AV. An adaptive geometry-based stochastic model for non-isotropic MIMO mobile-to-mobile channels. *IEEE Transactions on Wireless Communications* 2009; **8**(9): 4824–4835.
11. Jakes WC (ed.). *Microwave Mobile Communications*. IEEE Press: New Jersey, 1994.
12. Zheng YR, Xiao CS. Improved models for the generation of multiple uncorrelated Rayleigh fading waveforms. *IEEE Communication Letter* 2002; **6**(6): 256–258.
13. Youssef N, Wang C-X, Pätzold M. A study on the second order statistics of Nakagami-Hoyt mobile fading channels. *IEEE Transactions on Vehicular Technology* 2005; **54**(4): 1259–1265.
14. Wang C-X, Pätzold M, Yuan D. Accurate and efficient simulation of multiple uncorrelated Rayleigh fading waveforms. *IEEE Transactions on Wireless Communications* 2007; **6**(3): 833–839.
15. Wang C-X, Pätzold M, Yao Q. Stochastic modelling and simulation of frequency correlated wideband fading channels. *IEEE Transactions on Vehicular Technology* 2007; **56**(3): 1050–1063.

16. Wang C-X, Yuan D, Chen HH, Xu W. An improved deterministic SoS channel simulator for efficient simulation of multiple uncorrelated Rayleigh fading channels. *IEEE Transactions on Wireless Communications* 2008; **7**(9): 3307–3311.
17. Pätzold M, Wang C-X, Hogstad BO. Two new sum-of-sinusoids-based methods for the efficient generation of multiple uncorrelated Rayleigh fading channels, *IEEE Transactions on Wireless Communications* 2009; **8**(6): 3122–3131.
18. Patel CS, Stüber GL, Pratt TG. Simulation of Rayleigh-faded mobile-to-mobile communication channels. *Transactions on Communications* 2005; **53**(11): 1876–1884.
19. Wang R, Cox D. Channel modeling for ad hoc mobile wireless networks. *Proceedings of IEEE VTC'02-Spring*, Birmingham, USA, May 2002; pp. 21–25.
20. Zajić AG, Stüber GL. A new simulation model for mobile-to-mobile Rayleigh fading channels. *Proceedings IEEE WCNC'06*, Las Vegas, USA, April 2006; pp. 1266–1270.
21. Wang LC, Liu WC, YH Cheng. Statistical analysis of a mobile-to-mobile Rician fading channel model. *IEEE Transactions on Vehicular Technology* 2009; **58**(1): 32–38.
22. Zheng YR. A non-isotropic model for mobile-to-mobile fading channel simulations. *Proceedings IEEE MCC'06*, Washington, USA, October 2006; pp. 1–6.
23. Cheng X, Wang C-X, Laurenson DI. A generic space-time-frequency correlation model and its corresponding simulation model for MIMO wireless channels. *Proceedings of EuCAP'07*, Edinburgh, UK, November 2007; pp. 1–6.
24. Abdi A, Barger JA, Kaveh M. A parametric model for the distribution of the angle of arrival and the associated correlation function and power spectrum at the mobile station. *IEEE Transactions on Vehicular Technology* 2002 **51**(3): 425–434.
25. Gutiérrez CA, Pätzold M. Sum-of-sinusoid-based simulation of flat fading wireless propagation channels under non-isotropic scattering conditions. *Proceedings of IEEE GLOBECOM'07*, Washington, D.C., USA, November 2007; pp. 3842–3846.
26. Patel CS, Stüber GL, Pratt TG. Comparative analysis of statistical models for the simulation of Rayleigh faded cellular channels. *Transactions on Communications* 2005; **53**(6): 1017–1026.
27. Gradshteyn IS, Ryzhik IM. *Table of Integrals, Series, and Products* (5th edn), Jeffrey A (ed.). Academic: San Diego, CA, 1994.

AUTHORS' BIOGRAPHIES



Xiang Cheng (S'05) received B.Sc. and M.Eng. degrees in communication and information systems from Shandong University, China, in 2003 and 2006, respectively. Since October 2006, he has been a Ph.D. student at Heriot-Watt University, Edinburgh, U.K.

His current research interests include mobile propagation channel modeling, and simulation, multiple antenna technologies, mobile-to-mobile communications, and cooperative communications. He has published approximately 30 research papers in refereed journals and conference proceedings.

Mr Cheng was awarded the Postgraduate Research Prize from Heriot-Watt University in 2007 and 2008, respectively, for academic excellence and outstanding performance. He served as a TPC member for IEEE HPCC2008 and IEEE CMC2009.



Cheng-Xiang Wang (S'01-M'05-SM'08) received the B.Sc. and M.Eng. degrees in communication and information systems from Shandong University, China, in 1997 and 2000, respectively, and Ph.D. degree in wireless communications from Aalborg University, Denmark, in 2004.

Dr Wang has been a lecturer at Heriot-Watt University, Edinburgh, U.K. since 2005. He is also an honorary fellow of the University of Edinburgh, U.K., a guest researcher of Xidian University, China, and an adjunct professor of Guilin University of Electronic Technology, China. He was a research fellow at the University of Agder, Grimstad, Norway, from 2001–2005, a visiting researcher at Siemens AG-Mobile Phones, Munich, Germany, in 2004, and a research assistant at Technical University of Hamburg-Harburg, Hamburg, Germany, from 2000–2001. His current research interests include wireless channel modeling and simulation, error models, cognitive radio networks, vehicular communication networks, green radio communications, cooperative (relay) communications, cross-layer design of wireless networks, MIMO, OFDM, UWB, and 4G wireless communications and beyond. He has published one book chapter and over 120 papers in refereed journals and conference proceedings.

Dr Wang serves as an Editor for four international journals: *IEEE Transactions on Wireless Communications*, *Wireless Communications and Mobile Computing Journal* (John Wiley & Sons), *Security and Communication Networks Journal* (John Wiley & Sons), and *Journal of Computer Systems, Networks, and Communications* (Hindawi).

He is the leading Guest Editor for *IEEE Journal on Selected Areas in Communications*, *Special Issue on Vehicular Communications and Networks*. He served or is serving as a TPC member, TPC Chair, and General Chair for more than 40 international conferences. Dr Wang is listed in 'Dictionary of International Biography 2008 and 2009', 'Who's Who in the World 2008 and 2009', 'Great Minds of the 21st Century 2009', and '2009 Man of the Year'. He is a Senior Member of the IEEE, a member of the IET, and a Fellow of the HEA.



David I. Laurenson (M'90) is currently a Senior Lecturer at The University of Edinburgh, Scotland. His interests lie in mobile communications: at the link layer this includes measurements, analysis and modeling of channels, whilst at the network layer this includes provision of mobility management and Quality of Service support. His research extends to practical implementation of wireless networks to other research fields, such as prediction of fire spread using wireless sensor networks (<http://www.firegrid.org>), to deployment of communication networks for distributed control of power distribution networks. He is an associate editor for *Hindawi journals*, and acts as a TPC member for international communications conferences. He is a member of the IEEE and the IET.



Sana Salous (M'95) received B.E.E. degree from the American University of Beirut, Beirut, Lebanon, in 1978 and M.Sc. and Ph.D. degrees from the University of Birmingham, Birmingham, U.K., in 1979 and 1984, respectively. She was an Assistant Professor with Yarmouk University, Irbid, Jordan, until 1988 and a Research

Associate with the University of Liverpool, Liverpool, U.K., until 1989, at which point, she took up a lecturer post with the Department of Electronic and Electrical Engineering, University of Manchester Institute of Science and Technology (UMIST), Manchester, U.K. In 2003 she took up the Chair in Communications Engineering with the School of Engineering, Durham University, Durham, U.K, where she is currently the Director of the Centre for Communications Systems.



Athanasios V. Vasilakos (M'89) is currently Professor at the Dept. of Computer and Telecommunications Engineering, University of Western Macedonia, Greece, and Visiting Professor at the Graduate Programme of the Department of Electrical and Computer Engineering, National Technical University of Athens (NTUA). He is coauthor (with W. Pedrycz) of the books *Computational Intelligence in Telecommunications Networks* (CRC press, USA, 2001), *Ambient Intelligence, Wireless Networking, Ubiquitous Computing* (Artech House, USA, 2006), coauthor (with M. Parashar, S. Karnouskos, W. Pedrycz) *Autonomic Communications* (Springer, to appear), *Arts and Technologies* (MIT Press, to appear), coauthor (with Yan Zhang, Thrasylvoulos Spyropoulos) *Delay Tolerant Networking* (CRC press, to appear), coauthor (with M. Anastasopoulos) *Game Theory in Communication Systems* (IGI Inc, USA, to appear). He has published more than 200 articles in top international journals (i.e *IEEE/ACM Transactions on Networking*, *IEEE Transactions on Information Theory*, *IEEE JSAC*, *IEEE Transactions on Wireless Communications*, *IEEE Transactions on Neural Networks*, *IEEE Transactions on Systems, Man, and Cybernetics*, *IEEE T-ITB*, *IEEE T-CIAIG*, etc.) and conferences. He is the Editor-in-chief of the Inderscience Publishers journals: *International Journal of Adaptive and Autonomous Communications Systems* (IJAACS, <http://www.inderscience.com/ijaacs>), *International Journal of Arts and Technology* (IJART, <http://www.inderscience.com/ijart>). He was or is at the editorial board of more than 20 international journals including: *IEEE Communications Magazine* (1999–2002 and 2008–), *IEEE Transactions on Systems, Man and Cybernetics* (TSMC, Part B, 2007–), *IEEE Transactions on Wireless Communications* (invited), *IEEE Transactions on Information Theory in Biomedicine* (TITB, 2009–) etc. He chairs several conferences, e.g., ACM IWCMC'09, ICST/ACM Autonomics 2009. He is a chairman of the Telecommunications Task Force of the Intelligent Systems Applications Technical Committee (ISATC) of the IEEE Computational Intelligence Society (CIS). Senior Deputy Secretary-General and fellow member of ISIBM www.isibm.org (International Society of Intelligent Biological Medicine (ISIBM)). He is member of the IEEE and ACM.